











# Diffuse Calvarial Hyperostosis and Spontaneous Intracranial Hypotension: A Case-Control Study

 J.C. Babcock,  D.R. Johnson,  J.C. Benson,  D.K. Kim,  P.H. Luetmer,  D.P. Shlapak,  C.P. Cross,  M.P. Johnson,  J.K. Cutsforth-Gregory, and  C.M. Carr

## ABSTRACT

**BACKGROUND AND PURPOSE:** Diagnosing spontaneous intracranial hypotension and associated CSF leaks can be challenging, and additional supportive imaging findings would be useful to direct further evaluation. This retrospective study evaluated whether there was a difference in the prevalence of calvarial hyperostosis in a cohort of patients with spontaneous intracranial hypotension compared with an age- and sex-matched control population.

**MATERIALS AND METHODS:** Cross-sectional imaging (CT of the head or brain MR imaging examinations) for 166 patients with spontaneous intracranial hypotension and 321 matched controls was assessed by neuroradiologists blinded to the patient's clinical status. The readers qualitatively evaluated the presence of diffuse or layered calvarial hyperostosis and measured calvarial thickness in the axial and coronal planes.

**RESULTS:** A significant difference in the frequency of layered hyperostosis (31.9%, 53/166 subjects versus 5.0%, 16/321 controls,  $P < .001$ , OR = 11.58) as well as the frequency of overall (layered and diffuse) hyperostosis (38.6%, 64/166 subjects versus 13.2%, 42/321 controls,  $P < .001$ , OR = 4.66) was observed between groups. There was no significant difference in the frequency of diffuse hyperostosis between groups (6.6%, 11/166 subjects versus 8.2%, 26/321 controls,  $P = .465$ ). A significant difference was also found between groups for calvarial thickness measured in the axial ( $P < .001$ ) and coronal ( $P < .001$ ) planes.

**CONCLUSIONS:** Layered calvarial hyperostosis is more prevalent in spontaneous intracranial hypotension compared with the general population and can be used as an additional noninvasive brain imaging marker of spontaneous intracranial hypotension and an underlying spinal CSF leak.

**ABBREVIATION:** SIH = spontaneous intracranial hypotension

Spontaneous intracranial hypotension (SIH) classically presents with orthostatic headaches and results from a CSF leak in the absence of trauma or iatrogenic injury.<sup>1</sup> The CSF leak may arise from within the thecal sac, at the neural foramen, or just lateral to it in the case of CSF-venous fistulas and nerve root sleeve tears. Recently, imaging techniques such as digital subtraction myelography and CT dynamic myelography have improved the detection and localization of the dural tears and CSF-venous fistulas that cause SIH,<sup>2</sup> and effective treatments are available, including recently described endovascular techniques.<sup>3</sup> Unfortunately, SIH can be a challenging diagnosis because presenting symptoms vary widely.<sup>4</sup> In patients with equivocal clinical symptoms or radiographic evidence of SIH, additional supportive findings on conventional

imaging modalities would be useful to guide further imaging and clinical work-up. A recent study described an association between calvarial hyperostosis and SIH.<sup>5</sup> We performed a matched case-control study in a large group of patients with SIH to further investigate this association.

## MATERIALS AND METHODS

A retrospective case-control study was conducted following institutional review board approval with waived consent for Health Insurance Portability and Accountability Act compliance.

### Case Identification

Our institutional electronic medical record was queried to identify adult patients 18 years of age or older who underwent digital subtraction myelography, conventional myelography, or dynamic CT myelography for the indication of "CSF leak." The results of the query included patients who underwent one of the aforementioned imaging studies between May of 2018 (the time of the institution of the latest electronic medical record) and November

Received March 25, 2022; accepted after revision May 6.

From the Department of Radiology, Mayo Clinic, Rochester, Minnesota.

Please address correspondence to Jeffrey C. Babcock, MD, Department of Radiology, Mayo Clinic, 200 First St SW, Rochester, MN 55905; e-mail: BabcockJeffrey@mayo.edu

<http://dx.doi.org/10.3174/ajnr.A7557>

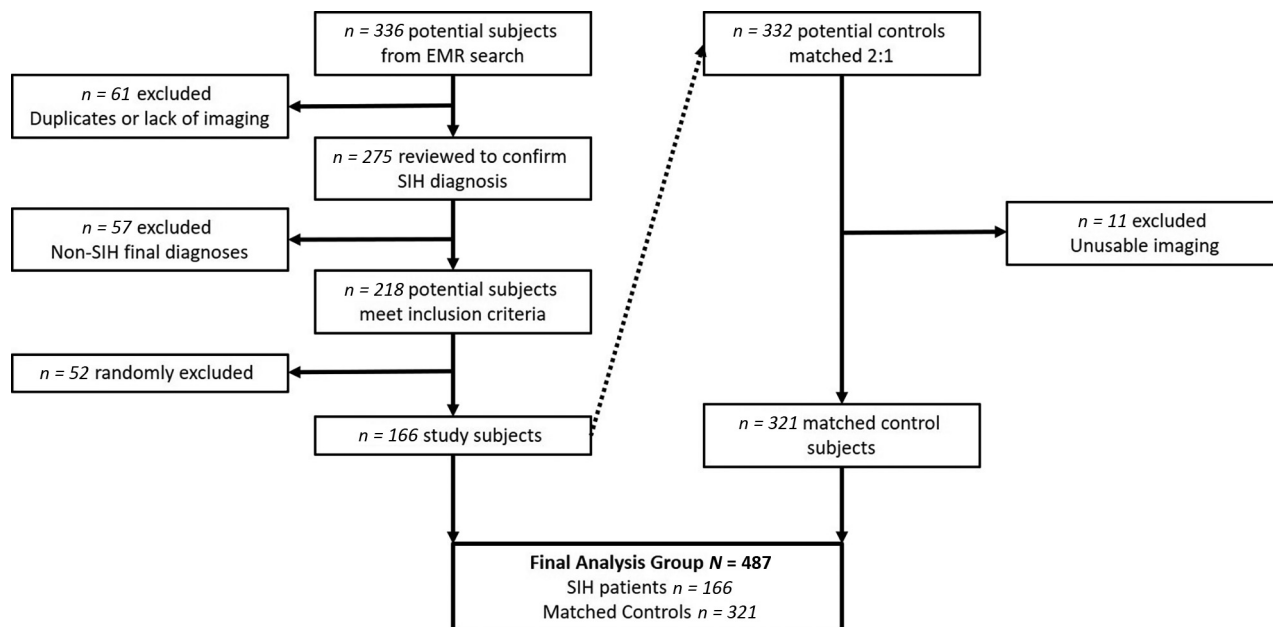


**FIG 1.** Flow chart defining the process of selecting the subject inclusion cohort. EMR indicates electronic medical record.

2020 (the time of the query). Only subjects with a final clinical diagnosis of SIH were included, as determined by 2 neurologists using modified diagnostic criteria supported by clinical history and radiographic findings in a fashion similar to that used in previous studies.<sup>6</sup> Patients without cross-sectional head imaging (CT or MR imaging) available for review and patients with a history suggestive of posttraumatic/postsurgical CSF leak or an alternative explanation of symptoms were excluded. This process identified 218 eligible cases, of which 166 were randomly selected to exceed the 157 cases needed per power calculations (Fig 1).

### Control Matching

Following the case-identification process, controls were matched 2:1 based on age, sex, and study type using the Greedy Matching Algorithm,<sup>7</sup> meaning that once a match was made it was never broken. All subjects were first matched to 1 control; then second control matching began. Sex and study type were matched exactly, and age was matched within 5 years. Study indication and disposition status varied among control examinations because the ability to match additional variables was limited. Available head imaging (CT or MR imaging) varied in the subject population, with either one or both available for each subject. The most recent available head imaging study was selected for analysis. If both MR imaging and CT were available in close succession, the CT head examination was preferentially selected for analysis to allow better spatial resolution and intrinsic contrast for the calvarial measurement. The matching process was designed to identify like control examinations for comparison (ie, CTs were matched to CTs, and MRIs to MRIs). If a control imaging study was found to be inadequate for analysis during image review, for example due to low-quality imaging in which hyperostosis could not be assessed, the control study was excluded and not replaced.

### Image Analysis

Six fellowship-trained neuroradiologists from our institution with experience ranging between 1 and 29 years postfellowship

evaluated the cases and controls for hyperostosis. An equal distribution of subject and control examinations was assigned to each neuroradiologist, randomized by a medical record number. All neuroradiologists were blinded to the control or subject status of each examination. Following predetermined instructions, each reader recorded 4 observations: 1) qualitative presence of diffuse hyperostosis (present or absent), 2) qualitative presence of layered hyperostosis (present or absent), 3) calvarial thickness measurement (millimeters) in the axial plane, and 4) calvarial thickness measurement (millimeters) in the coronal plane. Diffuse and layered hyperostosis was considered to be mutually exclusive.

Diffuse hyperostosis was subjectively identified by the presence of generalized thickening of the calvaria without discrete layering (Fig 2B). Layered hyperostosis can be thought of as a subtype of diffuse calvarial thickening in which there is distinct expansion of the inner bone table (Fig 2C), previously reported as having a “layer-cake” appearance.<sup>5</sup> To standardize calvarial thickness measurements, readers were given specific instructions. In the axial plane, maximal calvarial thickness was recorded at the level of the foramen of Monro 25°–35° off midline in either direction to avoid the frontal sinuses (Fig 3A, -B). In the coronal plane, a measurement was recorded where the calvaria was thickest 35°–45° off midline in either direction at the level of the vertex (Fig 3C, -D).

### Statistical Methods

This study was designed to achieve 80% power to detect an OR of 5 for calvarial hyperostosis in patients with SIH versus matched controls, assuming a type I error rate of 0.05 and estimating a 3% prevalence of calvarial hyperostosis in the general population. Using a 2:1 control-to-subject ratio, we determined that 157 subjects and 314 matched controls were required.

Patient characteristics for the analysis cohort, including a sample among matching variables, were summarized using percentage for categorical variables and mean (SD) for continuous

variables. Categorical variables were compared between groups using the Pearson  $\chi^2$  test, and continuous variables were compared using the 2-sample *t* test.

The association between calvarial hyperostosis and SIH was analyzed using conditional logistic regression to account for the matched data. *P* values < .05 were considered statistically significant. Sample size calculations were conducted using PASS 2021 (NCSS); matching was performed using SAS software, Version 9.4 (SAS Institute); and data analysis was completed using R, Version 3.6.2 (<http://www.r-project.org/>).

## RESULTS

### Patient Characteristics

There were no statistically significant differences in the mean patient age (*P* = .902), sex (*P* = .796), or examination type (*P* = .886) between the matched subject and control patient populations (Table 1). The median time from symptom onset to head imaging used for this study in the subject population was 26 months (interquartile range, 9–66). There was no statistically significant difference in the duration from symptom onset to the time of imaging among the SIH cohort based on the presence of diffuse hyperostosis, the presence of layered hyperostosis, or absence of hyperostosis (Table 2). Small numeric differences

between the matched cohorts resulted from subject exclusion, for example in the case of inadequate imaging.

### Subjective Hyperostosis Evaluation

Layered hyperostosis was present in 53/166 (31.9%) patients with SIH and 16/321 (5.0%) controls (*P* < .001). The OR for the presence of layered hyperostosis in patients with SIH in comparison with the control cohort was 11.58 (95% CI, 5.48–24.46). Diffuse hyperostosis was present in 11/166 (6.6%) patients with SIH and 26/321 (8.2%) controls (*P* = .46). The OR for the presence of diffuse hyperostosis in patients with SIH in comparison with the control cohort was 0.75 (95% CI, 0.36–1.59). Hyperostosis of either variety was present in 64/166 (38.6%) patients with SIH and 42/321 (13.2%) controls (*P* < .001). The OR for the presence of hyperostosis of either variety in patients with SIH in comparison with the control cohort was 4.66 (95% CI, 2.79–7.79). Two of 321 control images (0.6%) could not be assessed due to inadequate image resolution.

### Quantitative Calvarial Measurements

In the SIH patient group, the mean axial calvarial thickness was 7.3 (SD 2.6) mm with a range of 1.3–17.9 mm. In the control group, mean axial calvarial thickness was 6.4 (SD 1.9) mm with a range of 1.5–12.2 mm (*P* < .001, OR = 1.20; 95% CI, 1.09–1.32). Measurements of 1/166 (0.6%) patients with SIH and 2/321 (0.6%) control examinations could not be obtained due to inadequate image resolution.

With respect to coronal calvarial thickness, the mean measurement in patients with SIH was 7.4 (SD 2.0) mm with a range of 1.3–14.1 mm, and in the control group, the mean coronal calvarial thickness was 6.6 (SD 1.7) mm with a range of 2.6–13.9 mm (*P* < .001, OR = 1.32; 95% CI, 1.16–1.49). Fifty-five of 487 (11.2%) calvarial measurements could not be obtained due to the absence of a coronal plane in the image set or inadequate image resolution for retrospective reconstruction of coronal images; One of 166 (0.6%)

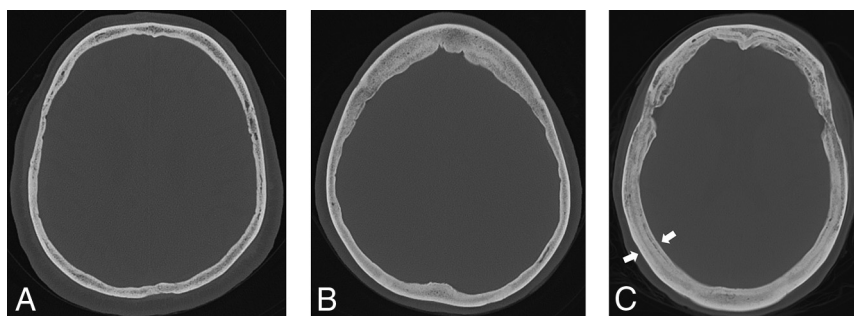


**FIG 2.** Hyperostosis examples. Normal calvarial thickness (A). Axial bone kernel and bone window CT image with a representative example of normal calvarial thickness. Diffuse calvarial hyperostosis (B). Axial bone kernel and bone window CT image demonstrates diffuse thickening of the calvaria. Layered calvarial hyperostosis (C). Axial bone kernel and bone window CT image demonstrates calvarial thickening with discrete enlargement of the inner and outer tables (white arrows), producing a layered appearance.

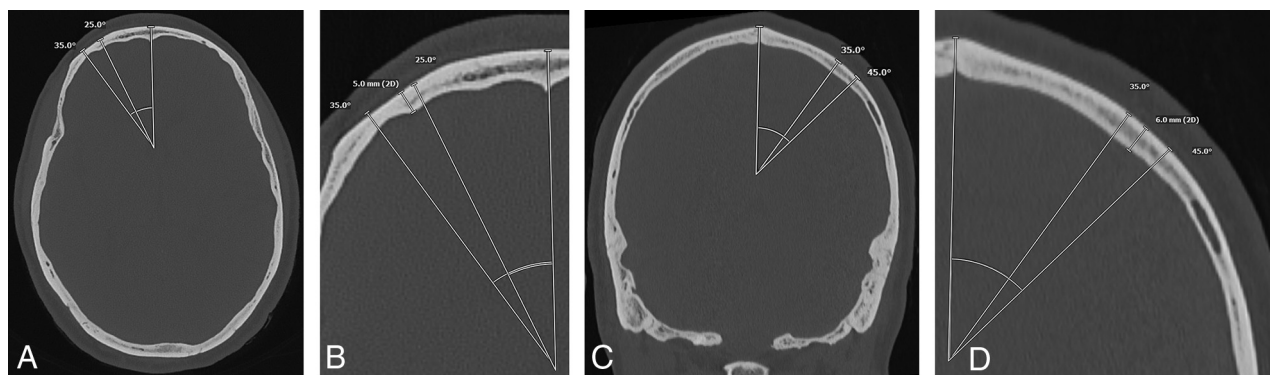


**FIG 3.** Example of calvarial thickness measurements obtained in the same patient in the axial and coronal planes. Full-field (A) and zoomed (B) axial bone kernel and bone window CT images demonstrate a sample axial thickness measurement obtained 25°–35° off midline. Full-field (C) and zoomed (D) coronal bone kernel and bone window CT images demonstrate a sample coronal thickness measurement obtained 35°–45° off midline.

patients and 54/321 (16.8%) control examinations were affected.

## DISCUSSION

This matched case-control study demonstrates that calvarial thickness differs between patients with SIH and the general population by both subjective and objective evaluation. Furthermore, our data indicate that the layer-cake phenotypic appearance is strongly associated with SIH, similar to prior observations,<sup>5</sup> approaching a frequency of nearly 1 in 3 in our population of patients with SIH, with an OR exceeding 11. Diffuse hyperostosis was not significantly associated with SIH in this study.

According to the Monro-Kellie hypothesis, the sum of intracranial CSF, blood, and brain parenchymal volumes must remain constant, and a change in one component necessitates reciprocal change in the others,<sup>8</sup> such as engorgement of the

venous structures or development of extra-axial fluid collections in response to a spinal CSF leak.<sup>9,10</sup> Classically, consideration of the Monro-Kellie hypothesis regards the overall intracranial volume as fixed and does not consider the calvaria as a distinct compartment that can potentially undergo change. Calvarial thickening, however, is a means by which the volume of the container could change in response to the loss of the interior contents.

The phenomenon of increased calvarial thickness has previously been reported in pediatric patients with ventricular shunts.<sup>11</sup> In 1 such case, Moseley et al<sup>12</sup> described calvarial remodeling with thickening of discrete inner and outer tables, analogous to the layer-cake appearance. We have observed notable change in calvarial thickness during serial examinations in some of our patients with SIH. One patient with chronic waxing and waning symptoms attributed to a spinal CSF leak developed calvarial thickening during 2 decades (Fig 4). The findings of this study support the phenomenon of increasing bone deposition specifically along the inner table of calvaria in the setting of intracranial volume loss, rather than generalized remodeling or thickening (diffuse hyperostosis pattern). However, the mechanism of this process remains unclear.

Rebound intracranial hypertension following successful treatment of various types of CSF leak may occur in about one-quarter of patients, most often within 1 week posttreatment, and it is generally self-limited in nature and responsive to acetazolamide.<sup>13</sup> The causes of rebound intracranial hypertension remain to be proven.<sup>14</sup> A new headache pattern despite improved or resolving imaging stigmata of CSF hypovolemia suggests rebound intracranial hypertension. Occasionally, papilledema may be appreciated by fundoscopy or MR imaging. While rare, rebound intracranial hypertension and papilledema can be prolonged in course and refractory to conservative measures. We have anecdotally observed multiple patients with hyperostosis developing severe rebound intracranial hypertension after successful treatment of a spinal CSF leak. One such patient with layered calvarial hyperostosis (Fig 5) ultimately required ventriculoperitoneal

shunt placement due to papilledema refractory to maximal acetazolamide and optic nerve sheath fenestration.

It may be valuable to further investigate the frequency of posttreatment rebound intracranial hypertension in patients with and without hyperostosis in a dedicated systemic study.

### Implications of Findings

SIH is often disabling, so it is gratifying to have improved imaging techniques for localizing spinal CSF leaks, such as CT dynamic myelography and digital subtraction myelography. Yet these examinations are invasive, uncomfortable, resource-intensive, and not available at many centers.<sup>9,15</sup> Because some

**Table 1: Subject and control group demographics**

	Subject (n = 166)	Control (n = 321)	P Value
Age (mean) (SD)	54.5 (12.8)	54.4 (12.9)	.902
Male sex	63 (38.0%)	118 (36.8%)	.796
CT studies	46 (27.7%)	87 (27.1%)	.886
MR imaging studies	120 (72.3%)	234 (72.9%)	

**Table 2: Symptom duration of the SIH cohort<sup>a</sup>**

	Present	Absent	P Value
Overall hyperostosis <sup>b</sup>	n = 64 36 months (12–78)	n = 102 22 months (8–49)	.171
Diffuse hyperostosis	n = 11 36 months (7–80)	n = 155 25 months (9–64)	.798
Layered hyperostosis	n = 53 36 months (12–77)	n = 113 22 months (8–51)	.197

<sup>a</sup>Numbers in parentheses are interquartile range (25<sup>th</sup> and 75<sup>th</sup> percentiles) of symptom duration in months.

<sup>b</sup>Diffuse and layered.

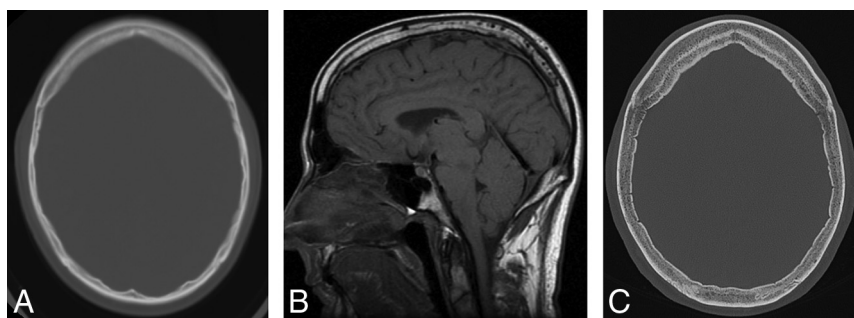


**FIG 4.** Development of hyperostosis in a 67-year-old man with 2 decades of waxing and waning SIH symptoms with a history of remote CSF leak at C2–C4. A, Axial CT head image at 45 years of age shows qualitatively normal calvarial thickness. B, Sagittal T1-weighted MR image at 48 years of age demonstrates severe brain sag and a suggestion of developing layered hyperostosis. Diffuse pachymeningeal thickening and enhancement are also present (not shown). C, The most recent axial head CT at 67 years of age demonstrates new layered calvarial hyperostosis.

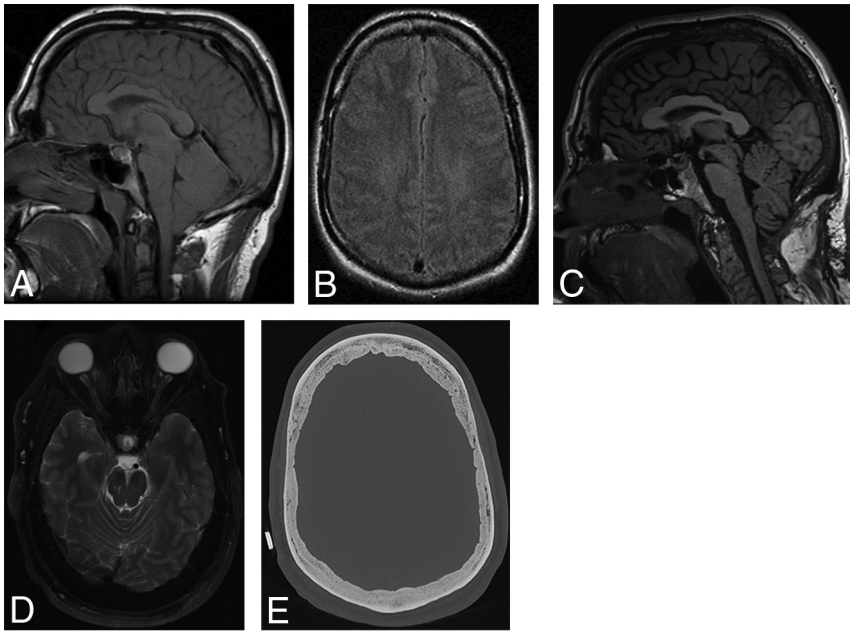


**FIG 5.** A 53-year-old man who developed refractory papilledema and rebound intracranial hypertension following repair of a CSF-venous fistula at T8–T9 at 51 years of age. Rebound intracranial hypertension symptoms began 3 weeks following treatment. Sagittal T1-weighted (A) and axial FLAIR (B) MR images at 29 years of age demonstrate brain sag with normal baseline qualitative calvarial thickness, respectively. Sagittal T1-weighted (C) and axial T2-weighted (D) MR images at 51 years of age demonstrate improvement in brain sag with new posterior globe flattening indicative of papilledema, respectively. E, Preoperative stereotactic CT image before ventriculoperitoneal shunt placement demonstrates new layered calvarial hyperostosis.

patients with spinal CSF leaks lack brain sag, pachymeningeal enhancement, and other classic signs of SIH, additional objective radiographic signs that increase the pretest probability of finding a leak and for selecting appropriate patients for invasive myelography are advantageous. Our study supports a relationship between layered calvarial hyperostosis and SIH, so in the proper clinical setting, it would be reasonable to offer further work-up for a CSF leak when layered calvarial hyperostosis is observed.

### Study Limitations

Although the neuroradiologists were blinded to the control-versus-subject status of the examination at the time of measurement, other qualitative imaging findings were sometimes present to suggest the diagnosis of SIH (eg, brain sag or pachymeningeal enhancement on MR imaging), potentially biasing the reader to presume a subject status. Due to limitations in the availability of a coronal plane or adequate resolution on some examinations (predominantly outside examinations), analysis was performed without many coronal plane calvarial measurements. Additionally, calvarial thickness in any given individual may be variable, possibly introducing measurement error despite a systematic approach in the study design. There is likely some degree of selection bias in the acquisition of the SIH inclusion cohort based on the indication of CSF leak when searching the myelogram imaging database. Additionally, it is plausible that our SIH cohort represents a

subselection of patients refractory to conservative treatment with longer symptom duration, given that we are a referral center. During the subject-to-control matching process, a small number of unsuitable control examinations (postoperative examinations or significant intracranial pathology) were matched and could not be used for analysis. Finally, although 6 neuroradiologists participated in this study, there was no formal analysis regarding interobserver agreement for subjective classification of diffuse or layered calvarial hyperostosis.

### CONCLUSIONS

Layered calvarial hyperostosis is present much more frequently in the setting of SIH than in the general population. In the proper clinical context, this finding should prompt further investigation for spinal CSF leak.

Disclosure forms provided by the authors are available with the full text and PDF of this article at [www.ajnr.org](http://www.ajnr.org).

### REFERENCES

- Schievink WI. Spontaneous intracranial hypotension. *N Engl J Med* 2021;385:2173–78 [CrossRef Medline](#)
- Schievink WI, Maya M, Prasad RS, et al. Spontaneous spinal cerebrospinal fluid-venous fistulas in patients with orthostatic headaches and normal conventional brain and spine imaging. *J Headache Pain* 2021;61:387–91 [CrossRef Medline](#)
- Brinjikji W, Savastano L, Atkinson J, et al. A novel endovascular therapy for CSF hypotension secondary to CSF-venous fistulas. *AJNR Am J Neuroradiol* 2021;42:882–87 [CrossRef Medline](#)
- Schievink WI. Spontaneous spinal cerebrospinal fluid leaks and intracranial hypotension. *JAMA* 2006;295:2286–96 [CrossRef Medline](#)
- Johnson DR, Carr CM, Luetmer PH, et al. Diffuse calvarial hyperostosis in patients with spontaneous intracranial hypotension. *World Neurosurg* 2021;146:e848–53 [CrossRef Medline](#)
- Schievink W, Maya M, Louy C, et al. Diagnostic criteria for spontaneous spinal CSF leaks and intracranial hypotension. *AJNR Am J Neuroradiol* 2008;29:853–56 [CrossRef Medline](#)
- Bergstrahl E, Kosanke J. Computerized Matching of Cases to Controls. Technical Report Number 56. *Mayo Foundation* 1995; 3:56
- Mokri B. The Monro-Kellie hypothesis: applications in CSF volume depletion. *Neurology* 2001;56:1746–48 [CrossRef Medline](#)
- Dobrocky T, Grunder L, Breiding PS, et al. Assessing spinal cerebrospinal fluid leaks in spontaneous intracranial hypotension with a scoring system based on brain magnetic resonance imaging findings. *JAMA Neurol* 2019;76:580–87 [CrossRef Medline](#)
- Dobrocky T, Rebsamen M, Rummel C, et al. Monro-Kellie hypothesis: increase of ventricular CSF volume after surgical closure of a spinal dural leak in patients with spontaneous intracranial hypotension. *AJNR Am J Neuroradiol* 2020;41:2055–61 [CrossRef Medline](#)

11. Lucey BP, March GP, Hutchins GM. **Marked calvarial thickening and dural changes following chronic ventricular shunting for shaken baby syndrome.** *Arch Pathol Lab Med* 2003;127:94–97 [CrossRef](#) [Medline](#)
12. Moseley JE, Rabinowitz JG, Dziadiw R. **Hyperostosis cranii ex vacuo.** *Radiology* 1966;87:1105–07 [CrossRef](#) [Medline](#)
13. Schievink WI, Maya MM, Jean-Pierre S, et al. **Rebound high-pressure headache after treatment of spontaneous intracranial hypotension.** *Neurol Clin Pract* 2019;9:93–100 [CrossRef](#) [Medline](#)
14. Mokri B. **Intracranial hypertension after treatment of spontaneous cerebrospinal fluid leaks.** *Mayo Clin Proc* 2002;77:1241–46 [CrossRef](#) [Medline](#)
15. Farb R, Nicholson P, Peng P, et al. **Spontaneous intracranial hypotension: a systematic imaging approach for CSF leak localization and management based on MRI and digital subtraction myelography.** *AJNR Am J Neuroradiol* 2019;40:745–53 [CrossRef](#) [Medline](#)